Blocker Protection by Short Spermine Analogs: Refined Mapping of the Spermine Binding Site in a Kir Channel

Harley T. Kurata,* Karthikeyan Diraviyam,† Laurence J. Marton,‡ and Colin G. Nichols*
*Department of Cell Biology and Physiology, †Center for Computational Biology, Washington University School of Medicine, St. Louis, Missouri; and ‡Progen Pharmaceuticals, Redwood City, California

ABSTRACT Strongly inwardly rectifying potassium channels are blocked by intracellular polyamines with a uniquely steep voltage dependence. An understanding of the fundamental details underlying the voltage dependence of polyamine block requires a constrained structural description of the polyamine-binding site. With this goal in mind, we previously used a "blocker protection" approach to examine the effects of polyamine occupancy on the rate of MTSEA modification of cysteine residues located at pore-lining sites in a strongly rectifying Kir channel (Kir6.2[N160D]). In the study presented here, we focused this strategy to characterize the effects of polyamine analogs that are similar in size to spermine on the rate of MTSEA modification. The observed protection profile of spermine is identical to that previously reported, with spermine occupancy inhibiting MTSEA modification of residue 157C, which is deep in the Kir pore, but having little effect on modification rates of 164C or 169C, closer to the intracellular side of the inner cavity. Remarkably, slightly longer synthetic spermine analogs (BE-spermine, CGC-11098) significantly increased the protection observed at position 164C. The extended protection profile observed with slightly extended polyamine analogs significantly enhances the resolution of our previous mapping efforts using the blocker protection approach, by eliminating uncertainties regarding the blocked conformations of the much longer polyamines that were used in earlier studies. For all short polyamine analogs examined, modification at the entrance to the inner cavity (169C) was unaffected by blocker occupancy, although blocker dissociation was dramatically slowed by partial modification of this site. These data support the validity of a blocker protection approach for mapping polyamine-binding sites in a Kir pore, and confirm that spermine binds stably at a deep site in the inner cavity of strongly rectifying Kir channels.

INTRODUCTION

Strong inward rectification of Kir channels involves voltage-dependent channel blockade by intracellular polycations such as putrescine, cadaverine, spermidine, and spermine (1–5). This process results in an apparent voltage dependence of channel activity, allowing robust K^+ currents to be carried in the inward direction at voltages more negative than the K^+ reversal potential, but little or no currents in the outward direction (6,7). Channels structurally classified as inward-rectifiers (within the KCNJ gene family) exhibit a range of rectification properties that depend significantly on the presence or absence of a negatively charged amino acid residue in the pore-lining M2 helix, referred to here as the ''rectification controller'' (7–11). Weakly rectifying channels typically lack a negatively charged residue in the inner cavity (e.g., Kir1.1 and Kir6.1/6.2), and are distinguished functionally by a weak affinity and shallow voltage dependence of polyamine block. Strongly rectifying channels (e.g., Kir2.1 and Kir6.2[N160D]) have a negatively charged ''rectification controller'', and the resulting steeply voltage-dependent polyamine block potently inhibits outward K^+ currents at depolarized voltages. The introduction of a negatively charged residue at any pore-lining position in a ''weak'' inward-rectifier (e.g., Kir6.2) is sufficient to confer highly potent and steeply voltage-dependent polyamine block, demonstrating the functional importance of the ''rectification controller'' (9,11,12). However, other channel-blocker interactions must also play a significant role, since neutralization of residue D172 in Kir2.1 channels does not abolish potent block by spermine (10,13, 14). In addition, some Kir3 channels exhibit relatively strong rectification properties despite the lack of a negatively charged residue in the inner cavity (15–17). Finally, mutations in the Kir channel cytoplasmic domain also influence the kinetics and steady-state properties of block by polyamines and other cations, such as Mg^{2+} (13,14,18–23).

As polyamines or other blockers traverse the Kir channel pore toward a stable binding site, a significant total charge is displaced, and this is reflected in the overall voltage dependence of blockade (1,6,24). This charge displacement arises at least in part from the movement of permeant ions coupled to movement of the blocking polyamine (25–27), but in addition the polyamine could contribute directly to the voltage dependence of block by traversing a small segment of the transmembrane field (11,28,29). A comprehensive description of inward rectification, and of Kir channel pore-blocking processes in general, will require a detailed understanding of ion binding sites and occupancy in the Kir pore, and a concrete description of stable blocker binding sites. With regard to spermine block of Kir channels, one group of studies argued for a model of ''shallow'' binding of spermine in the pore. With the exception of an early hint that the leading

Submitted March 11, 2008, and accepted for publication July 3, 2008.

Address reprint requests to Harley T. Kurata, Dept. of Cell Biology and Physiology, Washington University School of Medicine, 660 S. Euclid Ave., St. Louis, MO 63110. Tel.: 314-362-6629; Fax: 314-362-7463; E-mail: harley.kurata@wustl.edu.

Editor: Jian Yang.

0006-3495/08/10/3827/13 $2.00

doi: 10.1529/biophysj.108.133256

amine of spermine may extend slightly beyond the rectification controller (D172 in Kir2.1) (13), these studies have argued for a blocking configuration in which the leading amines of spermine are closely associated with the rectification controller (13,14,27). There was also a specific suggestion that the trailing amine of spermine interacts with Kir2.1 residue M183 (just outside the inner cavity, beyond the helix bundle-crossing region) (26). In contrast, other studies have suggested a deeper site for stable spermine binding, with the trailing amine interacting in the region of the rectification controller, and the leading amine extending toward and possibly even entering the selectivity filter (11,28–30). In this ''deep'' model of spermine binding, charged amines of the blocking polyamine may directly contribute some of the voltage dependence of blockade. A distinction between these two models will provide important constraints for future descriptions of the origins of voltage dependence in the mechanism of inward rectification, and of pore-blocking processes in general.

With the goal of determining the physical location of spermine block in Kir channels, we previously adopted a blocker protection approach in which we measured the inhibition of MTSEA modification of substituted cysteines in the presence of various blockers (28). In the presence of spermine, MTSEA modification at a very deep site in the pore was slowed, whereas the modification rates of residues closer to the intracellular side of the inner cavity were unaffected. This blocker protection profile could be extended to include a larger region of the inner cavity in the presence of a considerably longer polyamine analog (CGC-11179). Overall, these data supported a model of spermine binding deep in the Kir pore, between the rectification controller residue and the selectivity filter region. Nevertheless, due to the extremely large size of the extended polyamine probe (CGC-11179), some uncertainties arose regarding the effective spatial resolution of the approach. In the study presented here, we refined earlier blocker protection experiments to include synthetic polyamine analogs that differ more subtly in size from spermine (31). Importantly, the data demonstrate that even modest extensions of the spermine structure significantly change the protection profile in the Kir6.2 pore. These observations considerably enhance the resolution with which we can interpret blocker protection data, reinforcing the validity of the approach, and demonstrating that spermine likely binds at a very deep site in the Kir pore, predominantly between the rectification controller and selectivity filter.

MATERIALS AND METHODS

K_{ATP} channel constructs and expression in COSm6 cells

The experimental methods used in this study were described in detail in previous publications (32). The cysteine substitutions used (L157C, L164C, and M169C) were prepared by overlap extension at the junctions of relevant residues by sequential PCR on the Kir6.2 [C166S][N160D] background construct. The C166S mutation renders channels insensitive to Cd^{2+} or modification by MTSEA (32,33). In addition, C166S mutant channels are considerably more stable against rundown when compared to WT Kir6.2 channels, which is advantageous during long inside-out patch-clamp recordings (34). The N160D mutation confers steeply voltage-dependent, high-affinity binding of spermine and other polyamines.

Patch-clamp recording

COSm6 cells were transfected with 300 ng pCMV6b-Kir6.2 (with mutations as described), 500 ng pECE-SUR1, and 300 ng pGFP, using the Fugene 3.0 transfection reagent (Roche, Nutley, NJ). Patch-clamp experiments were performed at room temperature in a chamber that allowed the solution bathing the exposed surface of the isolated patch to be changed rapidly. Data were normally filtered at 0.5–2 kHz, and signals were digitized at 5 kHz and stored directly on a computer hard drive using Clampex software (Molecular Devices, Sunnyvale, CA). The standard pipette (extracellular) and bath (cytoplasmic) solution used in these experiments had the following composition: 140 mM KCl, 1 mM EGTA, 1 mM K_2-EDTA, 4 mM K_2HPO_4, pH 7. Spermine was purchased from FLUKA chemicals, Sigma-Aldrich, St. Louis, MO, and BE-spermine and CGC-11098 were made available to us through a collaboration with Progen Pharmaceuticals (Redwood City, CA). MTSEA and MTSES (Toronto Research Chemicals, North York, Canada) were dissolved in the standard recording solution on the day of experiments to make a 10 mM stock that was stored on ice. Further dilutions to 100 μM (or 500 μm for MTSES) were prepared and used immediately for channel modification.

Data analysis

The voltage dependence of blockade by spermine or analogs was fit with a Boltzmann function (Fig. 1 *E*): $\text{Grel} = 1/1 + \exp(z\delta F(V - V_{1/2})/RT)$, where F is Faraday's constant, R is the universal gas constant, T is temperature (298 K), and the fitted parameters are $z\delta$ (effective valence of block) and $V_{1/2}$ (the voltage at which 50% block is observed). The voltage-dependent time constants for dissociation of spermine or analogs were fit with a single exponential equation: $\tau\text{off} = \tau(0\text{ mV}) \times \exp(z\delta FV/RT)$. Current decay in the presence of MTSEA was fit empirically with a single exponential equation that included an offset (A) to account for incomplete inhibition of currents: $\text{Residual current} = (1 - A) \times \exp - (t/\tau) + A$. Fits were generated to individual data sets using Microsoft Solver with a least-squares algorithm to allow determination of standard errors for fitted parameters. Where applicable, data are presented as the mean ± SE.

Docking of polyamines in Kir6.2

A molecular model of an open conformation of Kir6.2[N160D] was generated as previously described for KirBac1.1 (35). Atomic models for polyamine blockers were constructed using Maestro molecular modeling software (Schrödinger, Portland, OR).

AutoDock 3.0 (36) was used to dock the various blockers on to the Kir6.2[N160D] homology model. The ion channel was treated as a rigid body and the blockers were treated as flexible, with conformations generated using an adaptive Lamarckian genetic algorithm (mutation rate: 0.02, crossover rate: 0.95). Multiple search spaces were used to identify binding sites: 1), the whole of the Kir6.2[N160D] protein; and 2), a restricted search space comprising the inner cavity and selectivity filter. All search spaces yielded similar predictions of polyamine binding sites, and sites outside the permeation pathway were omitted from the presented data or further consideration. Gasteiger partial charges were assigned to blockers, and hydrogen atoms were treated explicitly. One hundred docking runs were performed for each blocker in each search space. A grid spacing of 0.25 Å, with 10 million energy evaluations, and a starting population size of 100 were used. Resulting blocker conformations were clustered using a threshold root mean-square deviation of 6 Å.

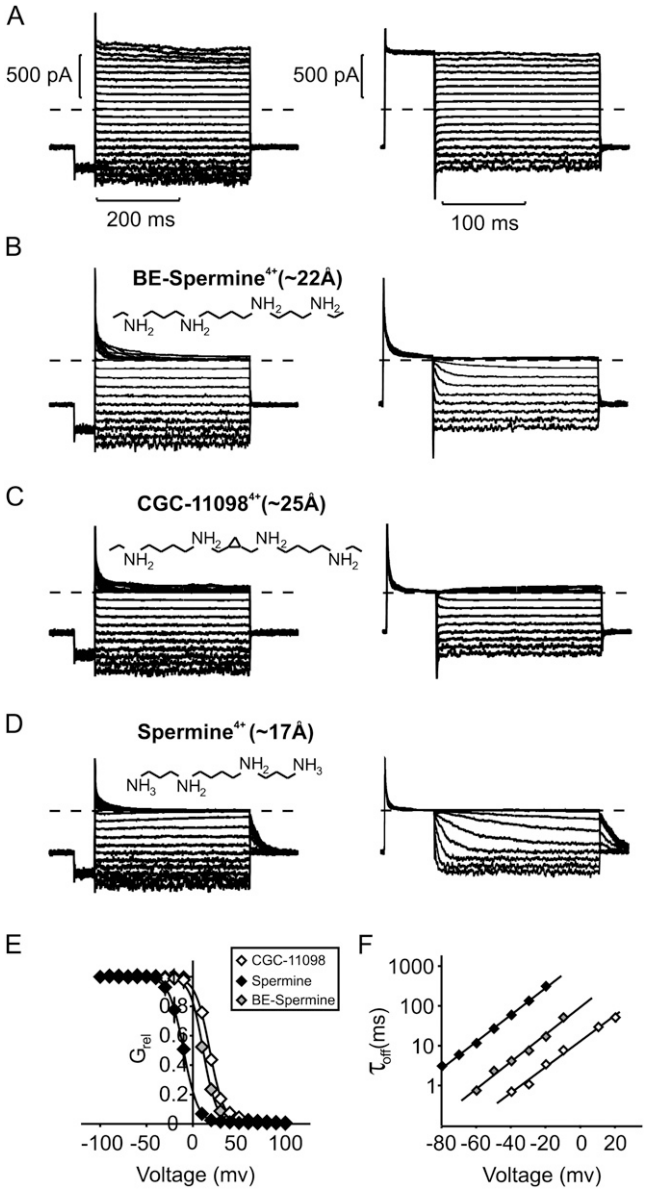

FIGURE 1 Blockade of Kir6.2[N160D][C166S] channels by spermine, BE-spermine, and CGC-11098. (*A–D*) BE-spermine, CGC-11098, and spermine were applied at a concentration of 10 μM to the intracellular side of inside-out patches excised from CosM6 cells expressing Kir6.2[N160D][C166S] channels (+SUR1). Two protocols were used to quantify blocking parameters. In the left panels (blocking protocol), patches were held at −50 mV, pulsed for 50 ms to −80 mV, and then pulsed for 400 ms to voltages between −100 mV and +100 mV. In the right panels (unblocking protocol), patches were held at –50 mV, pulsed for 50 ms to +80 mV, and repolarized for 200 ms to voltages between +80 mV and −80 mV in 10 mV steps. (*E*) Currents at voltages between −100 mV and +100 mV were normalized to currents in the absence of blockers (from panel *A*). Data are presented as mean ± SE (n = 5–7 patches per compound). Solid lines represent fitted Boltzmann functions for each blocker examined. (*F*) Off-rates of each blocker were measured by single exponential fits of the unbinding rates upon repolarization (unblocking protocol in panels *A–D*). Data are presented as mean ± SE (n = 5–7 per compound). Straight lines are single exponential fits of mean time constants of unblock.

RESULTS

Blocking properties of spermine, CGC-11098, and BE-spermine

We previously employed a ''blocker protection'' approach to investigate the polyamine-binding site in Kir channels (28). In the study presented here, we expanded this approach to include additional blockers that differ subtly in structure from spermine. The critical structural difference between spermine and the synthetic polyamines (Fig. 1, *B–D*) is the presence of bis-ethyl extensions on the terminal amines of CGC-11098 and BE-spermine. In addition, CGC-11098 is slightly (two additional carbon atoms) longer than BE-spermine, and has a conformationally restrictive cyclopropyl group between the second and third amines. Fully extended conformations of these synthetic polyamines have lengths (between terminal carbons) of 22 Å (BE-spermine) and 25 Å (CGC-11098), which are longer than that of spermine (17 Å between its terminal amines).

The blocking properties of spermine and the synthetic polyamines examined here have been reported in a previous study (31), but we revisit this topic briefly to confirm several critical points that are important for subsequent analysis and interpretation. In Kir6.2[N160D] channels, spermine exhibits a steeply voltage-dependent block ($z\delta \sim 4$, Fig. 1, *D* and *E*) that is comparable to spermine block of other strongly rectifying channels, including Kir2.1 and Kir4.1 (1,12,37). Both synthetic blockers examined here inhibit Kir6.2[N160D] channels with a very similar voltage dependence, which suggests that they reach a similar depth in the Kir6.2[N160D] channel pore (Fig. 1, *B*, *C*, and *E*). At a concentration of 10 μM, all three blockers inhibited channels with similar rates, although the potency of block was reduced for both BE-spermine and CGC-11098 relative to spermine (Fig. 1 *E*). Upon repolarization, BE-spermine and CGC-11098 unbound measurably faster than spermine (Fig. 1 *F*), which likely accounts for the observed reduction in blocker potency.

MTSEA modification of the Kir6.2 pore

As previously demonstrated by our group and others, overlap of a blocker with introduced cysteines can interfere with the rate of cysteine modification by methanethiosulfonate reagents—a phenomenon now commonly referred to as ''blocker protection'' (28,30,38–40). In the study presented here, we determined the blocker protection profile of spermine, CGC-11098, and BE-spermine in Kir6.2[N160D] channels with various substituted cysteine residues (L157C, L164C, and M169C) in the inner cavity. In the absence of any protecting blocker, MTSEA modification of cysteine residues substituted in the Kir6.2[N160D][C166S] pore causes an irreversible current reduction, with a characteristic time course (Fig. 2).

To determine the rate of MTSEA modification at +50 mV, excised patches were exposed to 100 μM MTSEA at a holding potential of +50 mV, with repeated brief repolari-

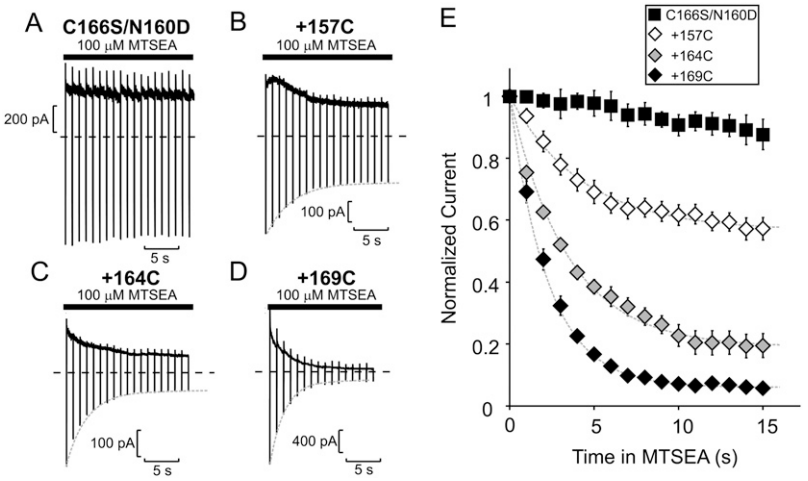

FIGURE 2 MTSEA modification of cysteine residues substituted in the Kir6.2 pore. (*A–D*) Sample data of modification of the Kir6.2 [N160D][C166S] background construct (*A*), with the (*B*) [L157C], (*C*) 164C, or (*D*) 169C mutations, by 100 μM MTSEA. To characterize the rate of MTSEA modification at +50 mV, patches were held at +50 mV after application of 100 μM MTSEA to the intracellular side of the patch and pulsed for 30 ms to −50 mV at 1 s intervals. (*E*) Mean data illustrating the modification time course of Kir6.2 [N160D][C166S][L157C], [L164C], and [M169C] channels by 100 μM MTSEA (n = 6–11 per data point). Dashed shaded lines (throughout the figures) represent monoexponential fits to the decay of current by MTSEA modification in the absence of any applied blocker.

zations to −50 mV at 1 s intervals. These brief repolarizations to −50 mV are sufficient to relieve MTSEA block, revealing the component of current reduction that is due to channel modification (33). Little or no current reduction is observed on the Kir6.2[N160D][C166S] background construct (Fig. 2, *A* and *E*). The overall time course of MTSEA-dependent current reduction in cysteine-substituted channels is well described by a monoexponential fit in each case (*dashed shaded lines* in Fig. 2, *B–E*).

Blocker protection at a deep site in the Kir6.2 pore

Blocker protection of substituted cysteines depends critically on both the location of the cysteine and the identity of the protecting blocker (28). Confirming our previous description of the blocker protection profile of spermine, channel inhibition by spermine significantly slowed MTSEA modification of L157C-substituted channels. Similar slowing of MTSEA modification was also observed with CGC-11098 and BE-spermine. Sample traces from typical experiments with all three blockers in the L157C channel are presented in Fig. 3, *A–C*. From a holding potential of −50 mV, patches were pulsed to +50 mV in the presence of 10 μM blocker. At the downward arrow, the patch was exposed to a solution containing 100 μM MTSEA in addition to 10 μM blocker. After a variable interval, patches were repolarized to −50 mV (to relieve block) and removed from the MTSEA-containing solution. Repolarization to −50 mV allowed measurement of the residual current after MTSEA exposure. In each case, the

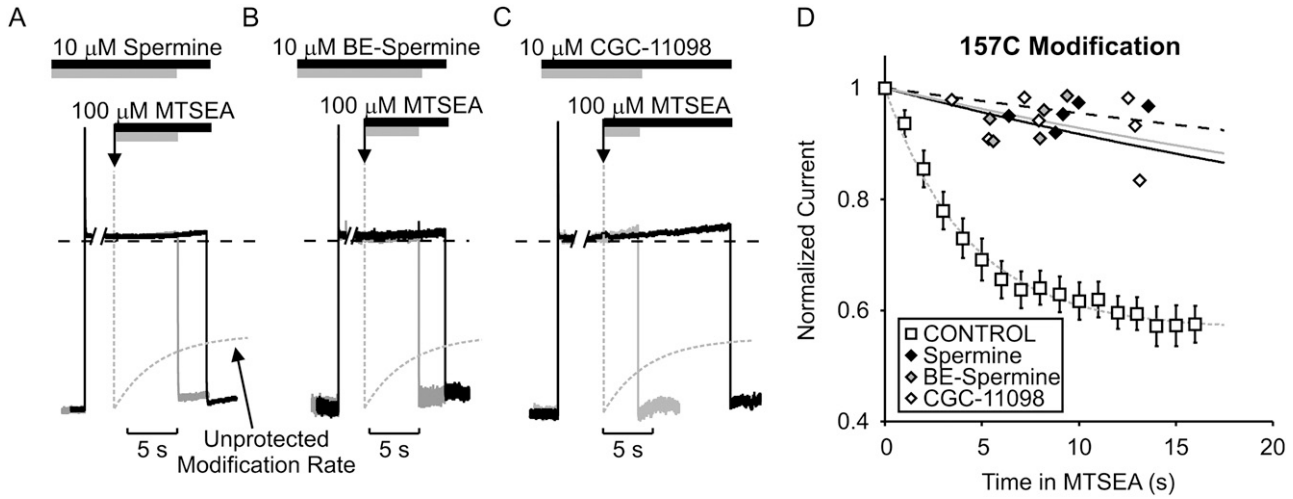

FIGURE 3 Protection of residue 157C by spermine, BE-spermine, or CGC-11098 occupancy of the Kir6.2 pore. Patches expressing Kir6.2[N160D][C166S][L157C] were blocked with voltage steps to +50 mV in either (*A*) 10 μM spermine, (*B*) 10 μM BE-spermine, or (*C*) 10 μM CGC-11098. While held continuously at +50 mV, patches were exposed to a solution containing the blocking polyamine + 100 μM MTSEA. After variable intervals in 100 μM MTSEA, patches were repolarized to −50 mV (to assess the extent of MTSEA modification) and immediately removed from the MTSEA-containing solution. The dashed shaded line represents the rate of MTSEA modification of L157C channels in polyamine-free conditions (from Fig. 2 *D*), and is superimposed on the raw data for comparison in each panel. (*D*) Modification of channels was measured in multiple patches after varying intervals in 100 μM MTSEA to determine the time course of modification when the pore is occupied by each polyamine (each data point represents a unique excised patch). Preblocking with either spermine, BE-spermine, or CGC-11098 strongly protects against MTSEA modification at residue 157C.

monoexponential fit (*dashed shaded line*) of the MTSEA modification rate in ''unprotected'' (i.e., unblocked) channels is superimposed on the raw data. Data from multiple patches are presented in Fig. 3 *D*. In L157C channels, a large residual current remained when channels were modified in the presence of spermine, CGC-11098, or BE-spermine (Fig. 3 *D*). Since modification of cysteines in the inner cavity can dramatically reduce blocker affinity, we discarded each patch after a single exposure to MTSEA, to eliminate possible confounding effects arising from MTSEA modification that could occur during periods when channels are unblocked. Thus each data point in Fig. 3 *D* represents a unique patch.

It should be noted that the blocker protection experiments were performed slightly differently from our previously described methodology (28) (discussed in more detail below). In previously published experiments, patches were exposed to MTSEA in a blocker-free solution after the channels were ''preblocked'' with a polyamine. In this study we included polyamine blockers in the MTSEA modification solution to maximize blocker occupancy during the modification step. The rationale for this slight modification was that the faster off-rates observed for BE-spermine and CGC-11098 (Fig. 1 *F*) could potentially confound interpretation of data. For example, if a blocker exhibits fast on/off kinetics, there is a possibility that an MTS reagent might enter and modify residues that overlap the blocker binding site during an interval in which the blocker has vacated the pore. In addition, we previously demonstrated that MTSEA modification at certain positions (especially 157C and 164C) can dramatically reduce polyamine affinity in Kir6.2[N160D] channels (11). The combination of these two effects could potentially cause a confounding false-negative result. The inclusion of blocker in the MTSEA modification solution minimizes the likelihood of this outcome by maximizing and sustaining blocker occupancy in the channel. Throughout this study, we also replicated our earlier blocker-protection examination of spermine with this revised protocol.

Extended blocker protection by short polyamine analogs

The fundamental novel finding reported here is that both CGC-11098 and BE-spermine, which are only slightly extended analogs of spermine, can considerably affect the outcome of the protection experiment. It is interesting that both considerably slow the MTSEA modification of residue 164C (Fig. 4). In raw data traces (Fig. 4, *A–C*) and in plots of data from multiple patches (Fig. 4 *D*), it is quite clear that MTSEA modification of 164C proceeds much more slowly in channels blocked by BE-spermine or CGC-11098, relative to unblocked channels or to channels occupied by spermine. As described for Fig. 3, each data point presented in Fig. 4 *D* was collected from a unique individual patch. Every patch that was modified while blocked by spermine (10 out of 10) exhibited considerably more current reduction during briefer MTSEA exposures compared to patches blocked by either CGC-11098 ($n = 10$) or BE-spermine ($n = 7$). This method to assess modification in the presence of a blocker is considerably more laborious than using a repetitive pulse protocol as described elsewhere; however, we believe it avoids certain caveats that may arise in these experiments. Most notably, differences in blocker kinetics relative to MTSEA may allow the modifying agent to enter and modify the inner cavity before a blocker has reached its binding site.

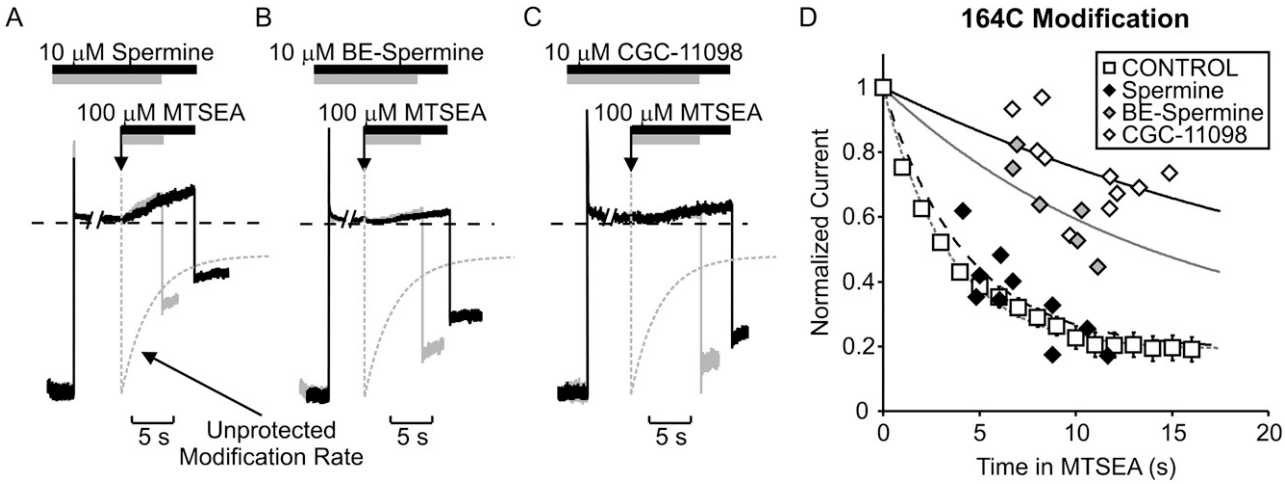

FIGURE 4 Short polyamines differentially protect residue 164C. Patches expressing Kir6.2[N160D][C166S][L164C] channels were blocked by voltage steps to +50 mV in either (*A*) 10 μM spermine, (*B*) 10 μM BE-spermine, or (*C*) 10 μM CGC-11098. As described in Fig. 4, patches were exposed to a solution containing the blocking polyamine + 100 μM MTSEA, where indicated by the downward arrow. After variable intervals in 100 μM MTSEA, patches were repolarized to −50 mV and immediately removed from the MTSEA-containing solution. (*D*) Modification of channels in the presence of each polyamine in multiple patches. Spermine occupancy does not prevent MTSEA modification of residue 164C, whereas BE-spermine and CGC-11098 both significantly decrease the rate of MTSEA modification at this position.

The findings are especially striking because the highest-affinity blocker (spermine) is the least effective at protecting position 164C. Importantly, differences in protection by spermine versus CGC-11098 or BE-spermine are immediately apparent in original experimental traces. When channels are blocked by spermine, application of MTSEA almost immediately initiates a relief of block by spermine (Fig. 4 *A*). A similar observation was made in our previous study (28), and we attribute this to a nearly unhindered modification of L164C leading to neutralization of nearby negative charges at N160D, resulting in a reduced spermine affinity. In contrast, this relief of block is much less apparent when channels are blocked with BE-spermine or CGC-11098 (Fig. 4, *B* and *C*), consistent with the assertion that MTSEA access to residue 164C is significantly more hindered by these extended blockers.

We also examined the protection of position 164C with a repetitive pulse protocol to better resolve the time dependence of modification in the presence of various blockers. In this experiment, patches were held at +50 mV with 100 μM MTSEA + 10 μM blocker, and briefly pulsed to −50 mV at 3-s intervals (Fig. 5). Importantly, this permits resolution of a modest protection of 164C by spermine that is not well resolved in Fig. 4 *D*. Nevertheless, a significant difference between spermine and BE-spermine/CGC-11098 is still obvious. For comparison, we have also included data for CGC-11179, a previously characterized blocker (28) that is significantly longer (fully extended length of ~46 Å) than the ''short'' spermine analogs used in study presented here. CGC-11179 protected 164C slightly more completely than BE-spermine or CGC-11098. The progressive relief of polyamine block noted in Fig. 4 was also apparent in the repetitive pulse experiment (Fig. 5 *A*), with outward currents developing more quickly in channels blocked by spermine versus CGC-11098, again consistent with weaker protection of position 164C by spermine. Finally, it should be noted that the time course of MTSEA modification in the presence of blockers does not appear to be described perfectly by a single exponential, but rather exhibits a brief delay. However, the deviations are not enormous, and we have not carefully characterized this feature of the data.

The negatively charged modifying reagent MTSES did not have any appreciable effect upon application to 164C channels (Fig. 6), and thus the contribution of electrostatic repulsion to the protection phenotype was not directly deduced. In *Shaker*, MTSES also had little effect on macroscopic conductance, but it caused a change in gating kinetics that could be used as an index of modification (39). Importantly, MTSES does not appear to access and modify the inner cavity of Kir6.2 channels, because subsequent application of cationic MTS reagents causes significant current reduction (Fig. 6, *A* and *B*). This demonstrates that cysteines in the inner cavity remain available for modification (i.e., unreacted) after membrane patch exposure to MTSES. The Kir channel pore is considerably longer than the Kv channel pore, and thus anions may be excluded more effectively from the inner cavity of Kir6.2.

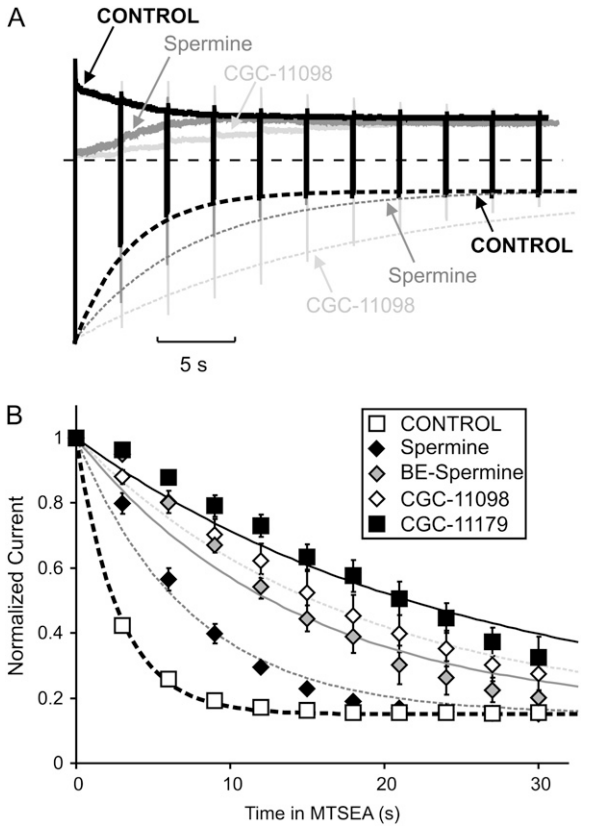

FIGURE 5 Time-resolved blocker protection of position 164C. Patches expressing Kir6.2[N160D][C166S][L164C] were exposed to 100 μM MTSEA in the presence of various blockers, held at +50 mV, and pulsed briefly to −50 mV at 3 s intervals. (*A*) Representative traces of patches modified in the presence of spermine (*shaded*) or CGC-11098 (*light shaded*), or the absence of blocker (*thick solid trace*). (*B*) Mean data illustrating MTSEA rundown in patches protected by various polyamine analogs (n = 4–6 per data point).

Slowed blocker unbinding after modification of 169C

In all cases, the short polyamine analogs fail to protect residue 169C. MTSEA modification occurs rapidly at position 169C, independently of the presence of any short polyamine blocker (Fig. 7, *A–D*). However, we previously observed that MTSEA modification of 169C, located in the helix bundle-crossing region (Fig. 8 *A*), dramatically slows both the blocking and unblocking rates for spermine (28). When channels are modified with spermine occupying the pore, a pronounced slow tail current is observed upon repolarization, corresponding to spermine release from modified channels. This unique feature of M169C modification illustrates not only the fact that spermine does not hinder MTSEA modification of M169C channels, but also that spermine can remain bound in the pore during the modification reaction. We observe similar features for BE-spermine and CGC-11098: the exit rate of these blockers is dramatically slowed after MTSEA modification. In the representative experiment in Fig. 8 *B*, a patch expressing

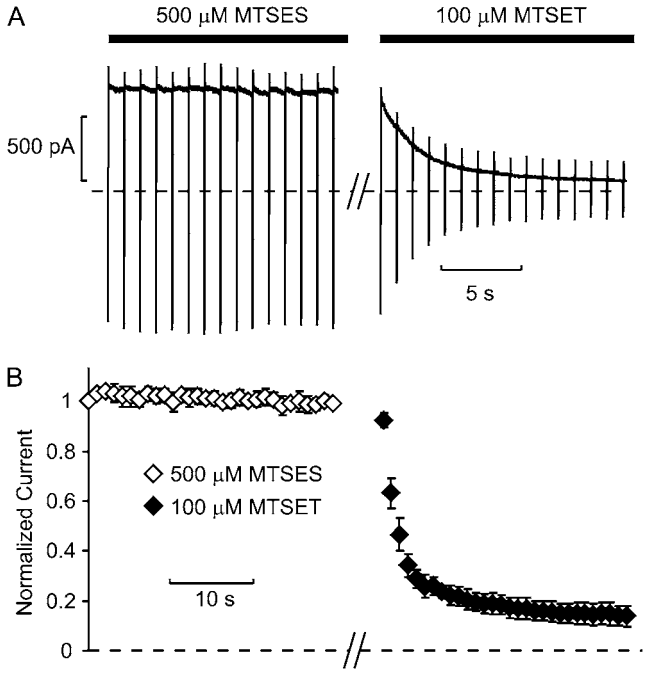

FIGURE 6 Modification of position 164C by MTSES. (*A*) Patches expressing Kir6.2[N160D][C166S][L164C] were exposed to 500 μM MTSES. Patches were held at +50 mV and briefly pulsed to −50 mV at 1 s intervals. No obvious effect on current magnitudes was observed. Patches were subsequently exposed to 100 μM MTSET, resulting in a substantial rundown of current, demonstrating that cysteines in the inner cavity were not modified by MTSES. (*B*) Mean data from multiple patches ($n = 3$).

M169C channels was first blocked in 10 μM spermine at +50 mV, then repolarized to −50 mV to observe the rate of polyamine unbinding from unmodified channels (*dashed gray box*). Channels were then blocked again, in 10 μM spermine at +50 mV, treated with 100 μM MTSEA (in the sustained presence of spermine), and repolarized to −50 mV to observe the rate of spermine unbinding from partially modified channels (*dashed black box*). Normalized tail currents from relevant segments of the experiment are shown for SPM (Fig. 8 *C*), BE-spermine (Fig. 8 *D*), and CGC-11098 (Fig. 8 *E*). Importantly, both BE-spermine and CGC-11098 have a faster unbinding rate than spermine in unmodified channels (Fig. 1 *F*). However, the similar effects of MTSEA modification of 169C on blocker unbinding for all three blockers indicates a qualitatively similar process.

Docking of short polyamine analogs in the Kir6.2 pore

Overall, the experimental data demonstrate a pattern of blocker protection in which spermine protects residue 157C, located above the rectification controller, whereas slightly extended forms of the blocker (BE-spermine and CGC-11098) can extend the protection profile to convincingly include residue 164C (one helical turn below the rectification controller). To examine the physical location of polyamine binding with an independent approach, we carried out a molecular docking exercise for all three polyamines, using a molecular model of the open conformation of Kir6.2[N160D] based on the open model of KirBac1.1 (35,41). This approach does not include a membrane voltage, or permeating potassium ions in the simulation. Rather, the docking runs are designed to identify the most stable interactions between the channel protein and blocker. In Fig. 9, the orange cloud indicates the volume occupied by all docking configurations identified by the simulation. A single space-filling model is depicted within each cloud (chosen from among the highest-ranked blocker conformations) that is consistent with our proposed location of polyamine binding. The predicted docked

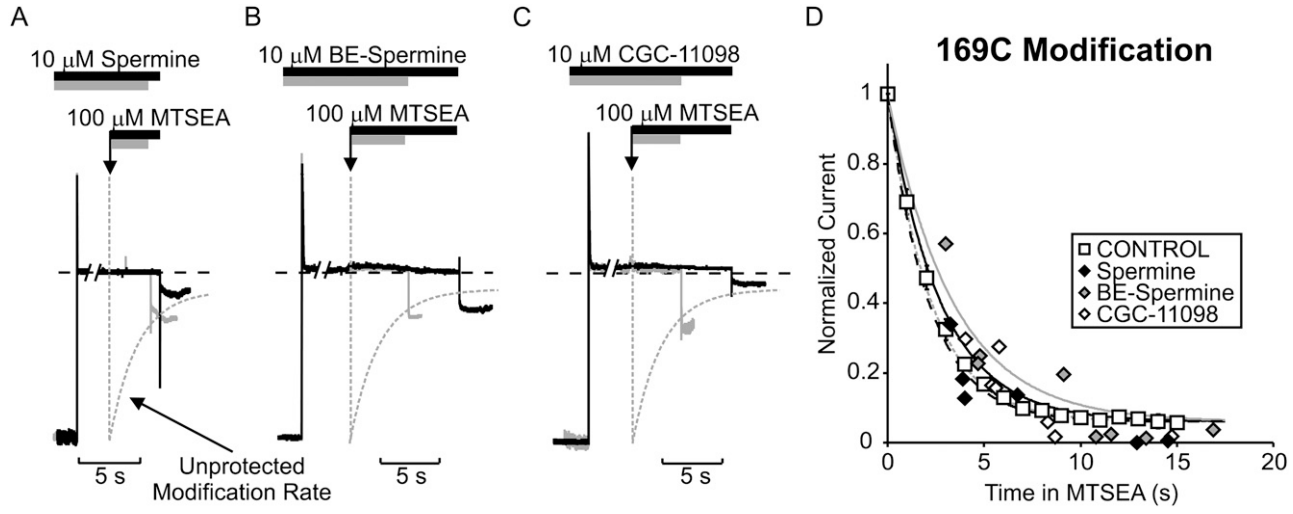

FIGURE 7 Residue 169C is not protected by short polyamines in the Kir6.2 pore. Patches expressing Kir6.2[N160D][C166S][M169C] were blocked by voltage steps to +50 mV in either (*A*) 10 μM spermine, (*B*) 10 μM BE-spermine, or (*C*) 10 μM CGC-11098, and exposed to a solution containing 100 μM MTSEA, as described in Figs. 3 and 4. (*D*) Modification of channels preblocked with each polyamine in multiple patches. Pore occupancy by the short polyamines examined does not significantly alter the rate of cysteine modification at 169C.

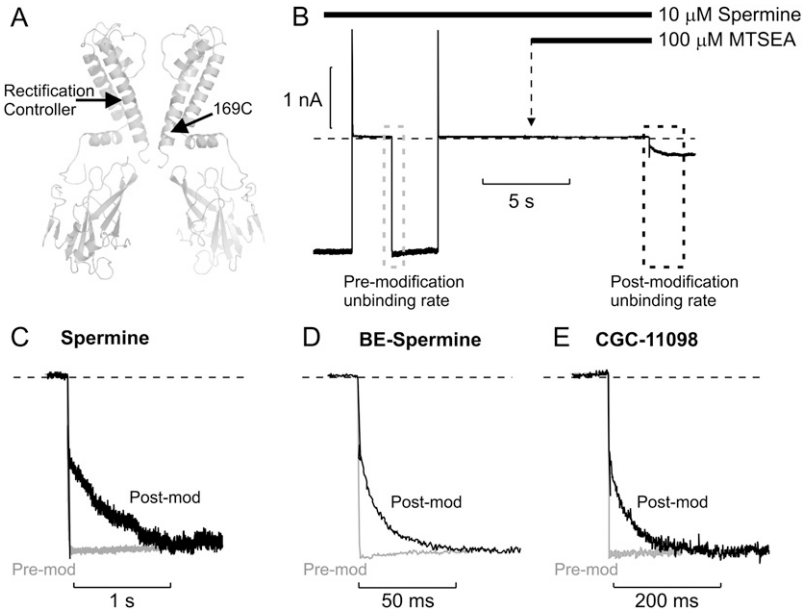

FIGURE 8 MTSEA modification of M169C ''traps'' short polyamines in the Kir6.2 pore. (*A*) Illustration of the location of residue 169C in the helix bundle-crossing region of Kir6.2, using the crystal structure of KirBac1.1 as a template. (*B*) Sample data of a blocker-protection experiment of Kir6.2[N160D][C166S][M169C] channels blocked with spermine. In this experiment, channels were first blocked with a pulse to +50 mV and then repolarized to −50 mV to observe the spermine unbinding rate from unmodified channels. In the second step, channels were blocked at +50 mV, and then exposed to a solution containing spermine + 100 μM MTSEA and repolarized to −50 mV to observe the spermine unbinding rate from partially modified channels. (*C–E*) Expanded data illustrating relevant tail currents observed in similar experiments using (*C*) spermine, (*D*) BE-spermine, or (*E*) CGC-11098. These data demonstrate that short spermine analogs can remain within the Kir6.2 pore during MTSEA modification of residue 169C, and that the introduction of positive charges at this site dramatically slows the dissociation rate of bound polyamines.

configurations of all three blockers examined cluster nearly exclusively in the volume between the rectification controller residue (colored orange) and the selectivity filter. Residues 157, 164, and 169 are highlighted in red, yellow, and green, respectively. We stress that the docking results alone should not be viewed as rigid predictors of polyamine binding sites, given that some determinants are not modeled. Furthermore, the docking runs employ a molecular model based on the KirBac1.1 open model, although a high-resolution structure of a Kir channel in the open state has not yet been described. Nevertheless, the docking results show good consistency with our experimental data, and also depict our conclusions and models of polyamine block with atomistic proportions.

DISCUSSION

Molecular details of polyamine block

Inward rectification of Kir channels arises from steeply voltage-dependent block by intracellular polyamines (1–3). With recent advances in our understanding of Kir channel structures at atomic resolution, and of specific potassium binding sites in K^+ channel pores (41–46), more detailed aspects of the mechanism of inward rectification can be addressed in particularly fine detail. The study presented here is focused primarily on localizing the stable binding site of spermine in a Kir pore, and assessing the viability of a blocker-protection approach for addressing this issue. At present, essentially two divergent models have been proposed to describe the location of stable spermine binding. Evidence presented by our group and others suggests a deep binding site for spermine in the inner cavity between the rectification controller residue and the selectivity filter (11,15,28–30), with the head of spermine lying near or within the selectivity filter. However, it has also been proposed that the leading amine(s) of spermine interact closely with the negatively charged ''rectification controller'' residue in the inner cavity (D172 in Kir2.1, equivalent to N160D in Kir6.2 examined in this study), with the trailing end extending toward and beyond the intracellular entrance to the inner cavity and interacting with Kir2.1 residue M183 (13,26,27).

Protection of the Kir6.2 inner cavity by polyamines

We previously mapped the spermine binding site to the external half of the inner cavity of Kir6.2[N160D] channels. We observed that spermine could hinder MTSEA modification of Kir6.2 residue 157C (in the external half of the cavity), but not residues 164C or 169C (closer to the cytoplasmic entrance of the inner cavity). In addition, the protected zone in the inner cavity could be extended if channels were blocked with a long polyamine analog (CGC-11179, ~46 Å in length, containing 10 amines; Fig. 10 *A*) (28). Although these findings provided strong evidence for a deep binding site for spermine, one acknowledged uncertainty/inconsistency arose from the observation that the length of the pore protected by CGC-11179 (residues 157C and 164C) was shorter than the fully extended length of the blocker. This could be a reflection of the conformation of the blocker in its bound state: CGC-11179 is extremely long, with dozens of bond torsions, and so it is possible that the blocker adopts a nonlinear conformation and leaves residue 169 unprotected (Fig. 10 *A*, *right panel*). A second possibility is that modifying reagents such as MTSEA might ''bypass'' the protecting blocker and reach some cysteines that overlap with the blocker binding site (Fig. 10 *A*, *left panel*). Without

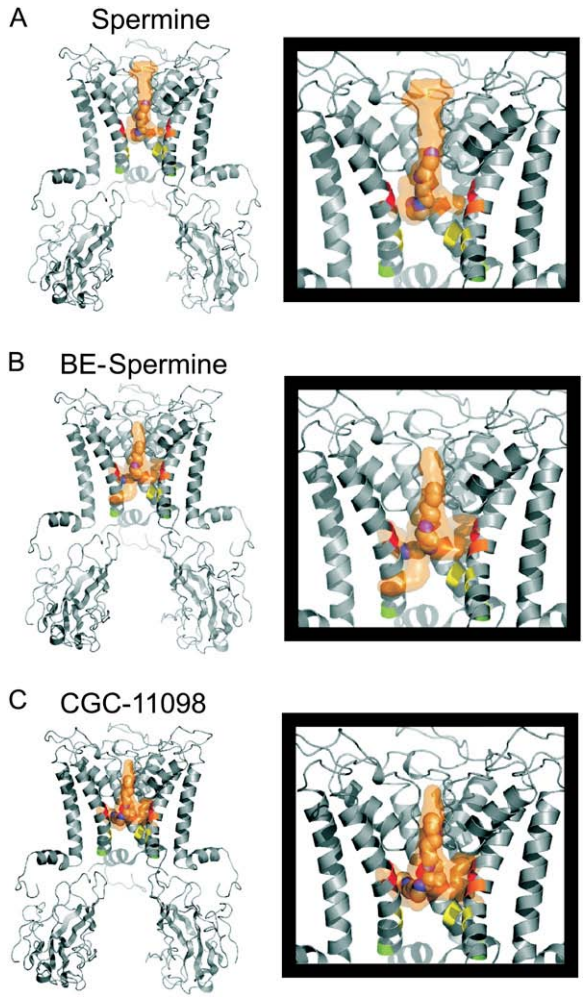

FIGURE 9 Docking of short spermine analogs in the Kir6.2[N160D] pore. A model of Kir6.2[N160D] similar to the open model of KirBac1.1 (35) was constructed. Using Autodock 3.0, structures of (*A*) spermine, (*B*) BE-spermine, and (*C*) CGC-11098 were docked into the model pore. The position of the rectification controller (residue 160D) is colored orange. Residues 157, 164, and 169 are colored red, yellow, and green, respectively. Several docking runs were performed for each blocker, with varied restrictions on the search space in the protein (the approximate search space for the depicted results comprised all of the inner cavity/selectivity filter, and ~2/3 of the volume within the cytoplasmic domain). The orange surface in each panel depicts the total volume occupied by all of the docked configurations generated by the program. Some individual configurations are predicted to be more favorable than others, but the overall view of the entire docking space demonstrates that the predicted configurations lie consistently between the rectification controller and the selectivity filter.

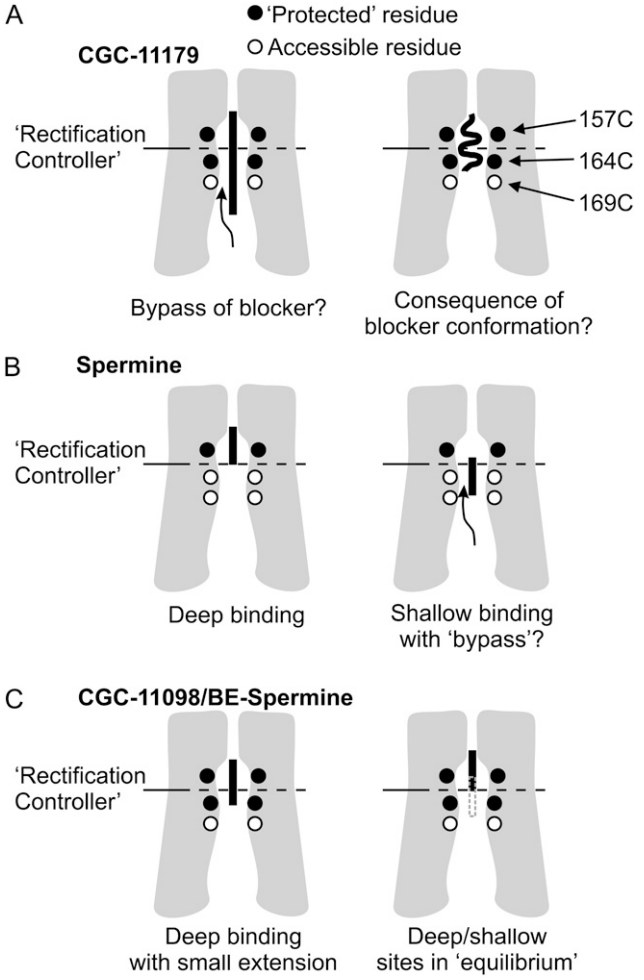

FIGURE 10 Physical interpretation of blocker protection in a Kir pore. Each panel is a cartoon depiction of our experimental system, with colored circles representing residues 157C, 164C, and 169C as indicated. The color of the circle reflects whether the corresponding residue is protected against MTSEA (*solid*) in a particular experiment, or not (*open*). In panel *A*, the long blocker CGC-11179 protects residues 157C and 164C, but not 169C. Since the protected zone is smaller than the fully extended length of the blocker, the protection profile could represent a compressed/coiled configuration of the blocker. A second possibility is ''bypass'' of the blocker by MTSEA, leading to modification of residues that overlap with the blocker-binding site. This ambiguity may cause uncertainty with regard to mapping the spermine-binding site, as depicted in panel *B*. Spermine protects only residue 157C, suggesting a deep binding site (*left panel*). However, if ''bypass'' is a possibility in the pore (*right panel*), spermine could potentially occupy a shallow binding site but remain unable to significantly protect 164C. The protection profiles observed for slightly extended spermine analogs (BE-spermine and CGC-11098) argue against this possibility. In the case of a shallow binding site with significant ''bypass'' (panel *B*, *right side*), slightly extended analogs should generate a protection profile similar to that of spermine. However, as schematized in *C*, both BE-spermine and CGC-11098 significantly inhibited modification of residue 164C (see also Figs. 4 and 5). We suggest two possible interpretations for this observation: One possibility is that slight extensions allow the spermine analogs to overlap with residue 164C and inhibit modification. A second possibility, consistent with the faster off-rate of these blockers, is that they flicker between the deep binding site and a slightly shallower site (indicated by *dotted shaded line* in Fig. 8 *C*, *right panel*), where blockers can prevent MTSEA occupancy and modification.

a convincing experimental tool to distinguish these two possibilities, we have argued that ''bypass'' is unlikely for several reasons. First, based on size and electrostatic repulsion, it seems unlikely that these compounds could move significantly past one another in the channel pore. Second, if significant ''bypass'' were taking place between MTSEA and a blocker, there is no strong rationale to explain the distinct boundaries of protection observed experimentally. For example, it is not apparent why MTSEA that has

''bypassed'' a fully extended linear blocker (as in the *left panel* of Fig. 10 *A*) would modify 169C but not 164C, or, for that matter, why MTSEA could ''bypass'' a linear spermine to reach 164C but not a linear CGC-11179. Finally, the blocker protection assay can be quite sensitive in that it provides a kinetic assessment of modification in the presence and absence of a blocker; therefore, even if a blocker fails to completely occlude a substituted cysteine (as in the ''bypass'' scenario), some difference in modification rate might be observed if access is hindered by interactions between the blocker and MTSEA.

Nevertheless, these ambiguities regarding conformations of long polyamine blockers, and the interaction of blockers and modifying reagents in the pore, leave room for debate regarding the interpretation of blocker-protection data. As discussed in the following sections, the experiments presented here refine the resolution of our previous blocker-protection study and support a model of spermine block at a deep site in the Kir pore between the ''rectification controller'' and selectivity filter (11,15,28–30).

Structural interpretations of blocker-protection profiles

The most critical and novel observation in this study is that even small extensions of the spermine structure can extend the profile of protected residues. Whereas spermine offers little protection against MTSEA modification of residue 164C, protection is more pronounced in channels blocked with either BE-spermine or CGC-11098 (Figs. 4 and 5). We can devise two plausible interpretations from these data, both of which are most consistent with the model of deep spermine binding between the rectification controller and the selectivity filter. A simple physical interpretation of these data is that slightly extended spermine analogs may occupy additional volume in the pore, extending slightly further toward the cytoplasmic entrance to the inner cavity, and hindering MTSEA occupancy at more shallow sites in the channel pore (Fig. 10 *C*, *left panel*). One drawback of this explanation is that docking runs predict stable blocker configurations clustered in the external half of the inner cavity for all three compounds (Fig. 9). Nevertheless, BE-spermine and CGC-11098 appear to occupy somewhat more volume around the rectification controller position. Also, since spermine and MTSEA compounds both carry positive charges at physiological pH, it is conceivable that protection of residue 164C could be generated by compounds occupying a deep position in the pore, due to mutual electrostatic repulsion between the blocker and modifying reagent.

A second potential explanation of these data stems from the observation that the extent of protection at position 164C seems to correlate inversely with the measured off-rate of each blocker; that is, CGC-11098, which exhibits the fastest off-rate of all three blockers examined (Fig. 1 *F*), and thus perhaps the lowest stability in the ''deep'' binding site, offers the most complete protection of residue 164C (Figs. 4 and 5). Spermine, in contrast, is the most potent of the three blockers, with the slowest off-rate, but offers the weakest protection at this position (Figs. 4 and 5). The bis-ethyl extended analogs may reside for briefer times in the deep site and exit with some frequency to a shallower site that effectively interferes with modification of 164C (Fig. 10 *C*, *right panel*). This would lead to the enhanced protection observed in the presence of CGC-11098 or BE-spermine. Importantly, the shallow position is likely to be above residue 169, because neither BE-spermine nor CGC-11098 is able to protect 169C, and dissociation of both compounds is considerably slowed by incorporation of positive charges at position 169C (Fig. 8, *D* and *E*).

Both suggested interpretations are fully consistent with the observed slowing of polyamine unbinding after modification of 169C, which demonstrates simultaneously that 1), MTSEA modification of 169C can occur (unhindered) with a polyamine occupying the pore; and 2), the introduction of positive charges at 169C heightens the energetic barrier for polyamine exit from the inner cavity. Collectively, the data argue that the most stable spermine-binding site lies at a deep location in the pore and does not overlap with either 164C or 169C.

Blocker/MTSEA interactions in the Kir pore

Importantly, this study addresses uncertainty arising in the conclusions from experiments with CGC-11179 (fully extended length ~46 Å). Using BE-spermine (~22 Å) and CGC-11098 (~25 Å), we have dramatically reduced the size of the probe required to observe protection of residue 164C, such that the protected region is now comparable in size to the blocker. Since a fully extended CGC-11179 would be predicted to overlap with residue 169C (but failed to protect this position) (28), we could not exclude the possibility that MTSEA can bypass blockers in the pore. As the size of the blocking probes is reduced, this possibility becomes more unlikely. For instance, if spermine resides primarily in a shallow blocking configuration (with unhindered modification of 164C arising due to ''bypass''; Fig. 10 *B*, *right panel*), modest extensions of spermine (e.g., BE-spermine) would have little effect.

It is worth noting that although we have argued that the ''bypass'' scenario is not likely, blockers are clearly able to exit from a partially modified 169C channel (which now has at least one ethylamine moiety permanently residing in the pore; Fig. 8). We view this as a unique scenario because freely diffusible MTSEA is of course considerably different from an immobilized ethylamine adduct, which can no longer diffuse in response to electrostatic repulsion from a nearby ion, and so it is inevitable that the blocker will eventually move past the modified cysteine in the pore. The demonstration that introduced positive charges dramatically hindered the movement of blockers (e.g., slowed off-rate, Fig. 8) and permeating ions (e.g., reduced macroscopic conduc-

tance) is fully consistent with our interpretation of the data, and suggests that an occupant blocker would significantly affect the kinetics of MTSEA access to an overlapping modification site.

Models of polyamine block in Kir channels: some common ground and divergent hypotheses

Overall, it is well understood that polyamine block of Kir channels involves multiple steps, and models comprising two blocking steps are sufficient to reproduce kinetic and steady-state features of polyamine block (5,23,27). Structurally, these are frequently interpreted to reflect ''shallow'' and ''deep'' blocking steps (21–23,27,29). The ''shallow'' step involves a weakly voltage-dependent association of polyamines with the cytoplasmic domain of the channel. This is followed by a ''deep'' blocking step, which is much more steeply voltage dependent, and involves movement of the blocking ion into a stable deep binding site. This study refines the structural details of the deep spermine-binding site in Kir channels.

As mentioned earlier, we recognize that some studies have presented a contrasting structural model of spermine block in which the leading amines are positioned in the vicinity of the rectification controller residue, and the trailing amine is positioned outside the inner cavity at residue M183 of Kir2.1 (equivalent to position 171 in Kir6.2) (13,26,27). Several findings of this study, and other previously published work, are inconsistent with this proposed model:

i. Position 169C: Clearly, neither spermine nor the bis-ethyl extended analogs (BE-spermine, CGC-11098, and CGC-11179) interfere with MTSEA modification of Kir6.2 residue 169C. Also, MTSEA modification does not affect spermine affinity at this position, suggesting that the stable spermine-binding site does not overlap with position 169C (11). Furthermore, modification at 169C clearly *slows* the unblocking kinetics of spermine and analogs (Fig. 8). These observations are wholly consistent with a model in which spermine resides entirely within the inner cavity, and modification of 169C generates a barrier for entry to/exit from the stable binding site.
ii. Position 164C: Protection of residue 164C is highly sensitive to the identity of the protecting blocker. Spermine exerts only modest effects on the rate of MTSEA modification at164C (28,30), whereas short extensions to spermine can significantly increase protection of residue 164C (Figs. 4 and 5). This marked sensitivity to the protecting blocker is consistent with 164C being at the boundary of the region of the inner cavity protected by spermine.
iii. Cysteines deep in the Kir pore: At deeper sites in the pore, including 157C and 129C (at the entrance to the selectivity filter), modification dramatically reduces spermine affinity and accelerates the spermine off-rate, consistent with these sites overlapping with the spermine binding site. Also, polyamine occupancy strongly protects both 157C and Kir2.1 residue 141C (equivalent to Kir6.2 129C) (40) against MTSEA modification.
iv. Insights into quaternary ammonium block arising from MTS modification of the Kir inner cavity: Consistent with a shallow spermine binding site, it has also been suggested that TEA block of Kir2.1 channels is localized to a peripheral site (specifically Kir2.1 residues E224 and E299) in the channel cytoplasmic domain (26). However, the ability of MTSEA and MTSET to modify cysteines in the inner cavity of Kir2.1 (and other Kir channels) suggests that ammonium and its quaternarized derivates can readily access deep sites in the inner cavity (11,28,30,47). Our own work in Kir6.2 has demonstrated that the voltage dependencies of TEA *block*, MTSEA *block*, and MTSEA *modification* of position 157C are comparable, suggesting that they all bind at the same place (around Kir6.2 residue 157), at the inner cavity ion binding/dehydration site (33). This is clearly consistent with the TEA binding site deduced functionally for *Shaker* and other Kv channels, and demonstrated crystallographically in KcsA channels (48,49).

Importantly, bis-QA-C10 (a 10-carbon diamine, with trimethylated terminal amines) appears to block Kir2.1 channels with an effective valence similar to that of spermine. This result supports the idea that much of the voltage dependence of spermine block arises from coupled movement of permeating ions (27), without the requirement that the blocking spermine ion enter the selectivity filter. One possible resolution of these findings with our own data is that the predicted charge associated with movement of a blocker from the cavity ion site into shallow sites in the filter (e.g., the S4 site) may be quite small, and thus predicted differences between certain models may be difficult to resolve in a patch-clamp experiment. Nevertheless, with studies such as the recent high-resolution crystallographic determination of a Kir channel (46), the understanding of permeant ion and blocker binding sites will continue to develop, and detailed models of coupled ion and blocker motions will help to resolve these issues.

CONCLUSIONS

In this study we have demonstrated that slightly extended spermine analogs (BE-spermine and CGC-11098) can expand the region of the inner cavity protected by spermine. Although different potential mechanisms may underlie this extended protection profile, all seem to be most consistent with a model of spermine binding at a deep site in the Kir pore. We are left to conclude that in its most stable bound state in a strongly rectifying Kir channel, spermine resides primarily between the rectification controller and selectivity filter.

We thank Sergey Noskov and Janice Robertson for early assistance with molecular models of the open Kir pore.

This work was supported by a grant from the National Institutes of Health (HL54171 to C.G.N.). H.T.K. was supported by a Canadian Institutes of Health Research Fellowship.

REFERENCES

1. Lopatin, A. N., E. N. Makhina, and C. G. Nichols. 1994. Potassium channel block by cytoplasmic polyamines as the mechanism of intrinsic rectification. *Nature*. 372:366–369.
2. Fakler, B., U. Brandle, E. Glowatzki, S. Weidemann, H. P. Zenner, and J. P. Ruppersberg. 1995. Strong voltage-dependent inward rectification of inward rectifier K+ channels is caused by intracellular spermine. *Cell*. 80:149–154.
3. Ficker, E., M. Taglialatela, B. A. Wible, C. M. Henley, and A. M. Brown. 1994. Spermine and spermidine as gating molecules for inward rectifier K+ channels. *Science*. 266:1068–1072.
4. Shyng, S. L., Q. Sha, T. Ferrigni, A. N. Lopatin, and C. G. Nichols. 1996. Depletion of intracellular polyamines relieves inward rectification of potassium channels. *Proc. Natl. Acad. Sci. USA*. 93:12014–12019.
5. Lopatin, A. N., E. N. Makhina, and C. G. Nichols. 1995. The mechanism of inward rectification of potassium channels: ''long-pore plugging'' by cytoplasmic polyamines. *J. Gen. Physiol.* 106:923–955.
6. Lopatin, A. N., and C. G. Nichols. 1996. [K+] dependence of polyamine-induced rectification in inward rectifier potassium channels (IRK1, Kir2.1). *J. Gen. Physiol*. 108:105–113.
7. Nichols, C. G., and A. N. Lopatin. 1997. Inward rectifier potassium channels. *Annu. Rev. Physiol.* 59:171–191.
8. Lu, Z., and R. MacKinnon. 1994. Electrostatic tuning of Mg2+ affinity in an inward-rectifier K+ channel. *Nature*. 371:243–246.
9. Lu, Z. 2004. Mechanism of rectification in inward-rectifier K+ channels. *Annu. Rev. Physiol.* 66:103–129.
10. Wible, B. A., M. Taglialatela, E. Ficker, and A. M. Brown. 1994. Gating of inwardly rectifying K+ channels localized to a single negatively charged residue. *Nature*. 371:246–249.
11. Kurata, H. T., L. R. Phillips, T. Rose, G. Loussouarn, S. Herlitze, H. Fritzenschaft, D. Enkvetchakul, C. G. Nichols, and T. Baukrowitz. 2004. Molecular basis of inward rectification: polyamine interaction sites located by combined channel and ligand mutagenesis. *J. Gen. Physiol.* 124:541–554.
12. Shyng, S., T. Ferrigni, and C. G. Nichols. 1997. Control of rectification and gating of cloned KATP channels by the Kir6.2 subunit. *J. Gen. Physiol.* 110:141–153.
13. Guo, D., and Z. Lu. 2003. Interaction mechanisms between polyamines and IRK1 inward rectifier K+ channels. *J. Gen. Physiol.* 122:485–500.
14. Guo, D., Y. Ramu, A. M. Klem, and Z. Lu. 2003. Mechanism of rectification in inward-rectifier K+ channels. *J. Gen. Physiol*. 121: 261–275.
15. Dibb, K. M., T. Rose, S. Y. Makary, T. W. Claydon, D. Enkvetchakul, R. Leach, C. G. Nichols, and M. R. Boyett. 2003. Molecular basis of ion selectivity, block, and rectification of the inward rectifier Kir3.1/Kir3.4 K(+) channel. *J. Biol. Chem.* 278:49537–49548.
16. Makary, S. M., T. W. Claydon, D. Enkvetchakul, C. G. Nichols, and M. R. Boyett. 2005. A difference in inward rectification and polyamine block and permeation between the Kir2.1 and Kir3.1/Kir3.4 K+ channels. *J. Physiol.* 568:749–766.
17. Makary, S. M., T. W. Claydon, K. M. Dibb, and M. R. Boyett. 2006. Base of pore loop is important for rectification, activation, permeation, and block of Kir3.1/Kir3.4. *Biophys. J.* 90:4018–4034.
18. Yang, J., Y. N. Jan, and L. Y. Jan. 1995. Control of rectification and permeation by residues in two distinct domains in an inward rectifier K+ channel. *Neuron*. 14:1047–1054.
19. Kubo, Y., and Y. Murata. 2001. Control of rectification and permeation by two distinct sites after the second transmembrane region in Kir2.1 K+ channel. *J. Physiol.* 531:645–660.
20. Fujiwara, Y., and Y. Kubo. 2006. Functional roles of charged amino acid residues on the wall of the cytoplasmic pore of Kir2.1. *J. Gen. Physiol.* 127:401–419.
21. Xie, L. H., S. A. John, and J. N. Weiss. 2003. Inward rectification by polyamines in mouse Kir2.1 channels: synergy between blocking components. *J. Physiol.* 550:67–82.
22. Xie, L. H., S. A. John, and J. N. Weiss. 2002. Spermine block of the strong inward rectifier potassium channel Kir2.1: dual roles of surface charge screening and pore block. *J. Gen. Physiol.* 120:53–66.
23. Kurata, H. T., W. W. Cheng, C. Arrabit, P. A. Slesinger, and C. G. Nichols. 2007. The role of the cytoplasmic pore in inward rectification of Kir2.1 channels. *J. Gen. Physiol.* 130:145–155.
24. Guo, D., and Z. Lu. 2000. Mechanism of IRK1 channel block by intracellular polyamines. *J. Gen. Physiol*. 115:799–814.
25. Spassova, M., and Z. Lu. 1998. Coupled ion movement underlies rectification in an inward-rectifier K+ channel. *J. Gen. Physiol.* 112: 211–221.
26. Shin, H. G., Y. Xu, and Z. Lu. 2005. Evidence for sequential ion-binding loci along the inner pore of the IRK1 inward-rectifier K+ channel. *J. Gen. Physiol*. 126:123–135.
27. Shin, H. G., and Z. Lu. 2005. Mechanism of the voltage sensitivity of IRK1 inward-rectifier K+ channel block by the polyamine spermine. *J. Gen. Physiol.* 125:413–426.
28. Kurata, H. T., L. J. Marton, and C. G. Nichols. 2006. The polyamine binding site in inward rectifier k+ channels. *J. Gen. Physiol*. 127:467–480.
29. John, S. A., L. H. Xie, and J. N. Weiss. 2004. Mechanism of inward rectification in Kir channels. *J. Gen. Physiol.* 123:623–625.
30. Chang, H. K., S. H. Yeh, and R. C. Shieh. 2003. The effects of spermine on the accessibility of residues in the M2 segment of Kir2.1 channels expressed in *Xenopus* oocytes. *J. Physiol.* 553:101–112.
31. Loussouarn, G., L. J. Marton, and C. G. Nichols. 2005. Molecular basis of inward rectification: structural features of the blocker defined by extended polyamine analogs. *Mol. Pharmacol.* 68:298–304.
32. Loussouarn, G., E. N. Makhina, T. Rose, and C. G. Nichols. 2000. Structure and dynamics of the pore of inwardly rectifying K(ATP) channels. *J. Biol. Chem.* 275:1137–1144.
33. Phillips, L. R., D. Enkvetchakul, and C. G. Nichols. 2003. Gating dependence of inner pore access in inward rectifier K(+) channels. *Neuron*. 37:953–962.
34. Trapp, S., P. Proks, S. J. Tucker, and F. M. Ashcroft. 1998. Molecular analysis of ATP-sensitive K channel gating and implications for channel inhibition by ATP. *J. Gen. Physiol.* 112:333–349.
35. Domene, C., D. A. Doyle, and C. Venien-Bryan. 2005. Modeling of an ion channel in its open conformation. *Biophys. J.* 89:L01–L03.
36. Morris, G. M., D. S. Goodsell, R. S. Halliday, R. Huey, W. E. Hart, R. K. Belew, and A. J. Olsen. 1998. Automated docking using a Lamarckian genetic algorithm and and empirical binding free energy function. *J. Comput. Chem.* 19:1639–1662.
37. Oliver, D., H. Hahn, C. Antz, J. P. Ruppersberg, and B. Fakler. 1998. Interaction of permeant and blocking ions in cloned inward-rectifier K+ channels. *Biophys. J.* 74:2318–2326.
38. Andalib, P., J. F. Consiglio, J. G. Trapani, and S. J. Korn. 2004. The external TEA binding site and C-type inactivation in voltage-gated potassium channels. *Biophys. J.* 87:3148–3161.
39. Del Camino, D., M. Holmgren, Y. Liu, and G. Yellen. 2000. Blocker protection in the pore of a voltage-gated K+ channel and its structural implications. *Nature*. 403:321–325.
40. Yeh, S. H., H. K. Chang, and R. C. Shieh. 2005. Electrostatics in the cytoplasmic pore produce intrinsic inward rectification in kir2.1 channels. *J. Gen. Physiol.* 126:551–562.

41. Kuo, A., C. Domene, L. N. Johnson, D. A. Doyle, and C. Venien-Bryan. 2005. Two different conformational states of the KirBac3.1 potassium channel revealed by electron crystallography. *Structure*. 13: 1463–1472.

42. Nishida, M., and R. MacKinnon. 2002. Structural basis of inward rectification: cytoplasmic pore of the G protein-gated inward rectifier GIRK1 at 1.8 A resolution. *Cell*. 111:957–965.

43. Kuo, A., J. M. Gulbis, J. F. Antcliff, T. Rahman, E. D. Lowe, J. Zimmer, J. Cuthbertson, F. M. Ashcroft, T. Ezaki, and D. A. Doyle. 2003. Crystal structure of the potassium channel KirBac1.1 in the closed state. *Science*. 300:1922–1926.

44. Pegan, S., C. Arrabit, W. Zhou, W. Kwiatkowski, A. Collins, P. A. Slesinger, and S. Choe. 2005. Cytoplasmic domain structures of Kir2.1 and Kir3.1 show sites for modulating gating and rectification. *Nat. Neurosci*. 8:279–287.

45. Inanobe, A., T. Matsuura, A. Nakagawa, and Y. Kurachi. 2007. Structural diversity in the cytoplasmic region of G protein-gated inward rectifier K+ channels. *Channels*. 1:39–45.

46. Nishida, M., M. Cadene, B. T. Chait, and R. MacKinnon. 2007. Crystal structure of a Kir3.1-prokaryotic Kir channel chimera. *EMBO J*. 26: 4005–4015.

47. Lu, T., B. Nguyen, X. Zhang, and J. Yang. 1999. Architecture of a K+ channel inner pore revealed by stoichiometric covalent modification. *Neuron*. 22:571–580.

48. Zhou, M., J. H. Morais-Cabral, S. Mann, and R. MacKinnon. 2001. Potassium channel receptor site for the inactivation gate and quaternary amine inhibitors. *Nature*. 411:657–661.

49. Yellen, G., M. E. Jurman, T. Abramson, and R. MacKinnon. 1991. Mutations affecting internal TEA blockade identify the probable pore-forming region of a K^+ channel. *Science*. 251:939–942.